Journal of Non-Crystalline Solids 358 (2012) 2052–2056

Contents lists available at SciVerse ScienceDirect

Journal of Non-Crystalline Solids

journal homepage: www.elsevier.com/ locate/ jnoncrysol

a-Si:H transport parameters from experiments based on photoconductivity

C. Longeaud [a,*], J.A. Schmidt [b]

[a] Laboratoire de Génie Electrique de Paris (CNRS UMR 8507), Plateau de Moulon, 11 rue Joliot Curie, 91190 Gif sur Yvette, France
[b] INTEC (UNL-CONICET), Güemes 3450, 3000 Santa Fe, Argentina

ARTICLE INFO

Article history:
Received 9 June 2011
Received in revised form 3 November 2011
Available online 10 December 2011

Keywords:
Hydrogenated amorphous silicon;
Transport parameters;
Photoconductivity;
Density of states

ABSTRACT

In this paper we review some of the techniques based on the photoconductivity property of hydrogenated amorphous silicon (a-Si:H) from which it is possible to extract transport parameters as well as density of states (DOS) spectroscopies. We also present a new experiment based on the steady state photocarrier grating technique. We show that combined with simple steady state photoconductivity it gives information on the DOS. The comparison of these results with those of other techniques used for DOS measurements theoretically allows determination of transport parameters in a-Si:H.

1. Introduction

Hydrogenated amorphous silicon (a-Si:H) is one of the major thin film materials used for solar energy conversion and lots of researches have been carried on for measuring its transport parameters to optimize the deposition conditions and its properties. Several techniques developed to determine a-Si:H transport parameters are based on its photoconductivity property and only the light excitation spatial and temporal distributions are varied from one experiment to the other. Considering the subset of experiments in which carrier generation is achieved by band to band excitation we can quote the following methods. The simplest one is the steady-state photoconductivity (SSPC) in which one records the evolution of the film photoconductivity with temperature T and/or generation rate G. More sophisticated techniques were designed as the modulated photocurrent (MPC) technique [1]. Other experiments are based on illuminating the film with interferences created by two laser beams. The grating can be fixed as in the steady state photocarrier grating (SSPG) [2], moving at a constant velocity along the film surface [3], or be modulated at a given frequency [4]. Each of these techniques brings some insight on the transport parameters and/or density of states (DOS) of the studied thin film.

In this paper we review some of them and show what information they bring and how complementary they are. Besides, we propose a new method, we show which information can be extracted from it, and demonstrate that an accurate DOS spectroscopy can be done with it. Combined with MPC it should also lead to the determination of important parameters as the electronic extended states mobility μ_n.

2. Experiments

2.1. Theoretical background

The MPC technique was first proposed by Oheda [1]. Basically, the sample is illuminated by a light flux, modulated at an angular frequency ω, giving an expression of $G = G_{dc} + G_{ac}\cos(\omega t)$, where the indexes *dc* and *ac* stand for steady and alternating components and $G_{ac} << G_{dc}$. Starting from the continuity equations, and after some calculations, one finally finds that [5,6]

$$\frac{N(E_\omega)c_n}{\mu_n} = \frac{2}{\pi k_B T} q G_{ac} \frac{\sin\phi}{|\sigma_{ac}|} \tag{1}$$

with

$$E_c - E_\omega = k_B T \ln\left(\frac{c_n N_c}{\omega}\right), \tag{2}$$

where k_B is the Boltzmann constant, q the electron charge, $N(E_\omega)$ the DOS at the energy E_ω, c_n the electron capture coefficient of the states at E_ω, E_c the conduction band edge energy, N_c the equivalent density of states at E_c, σ_{ac} the modulus of the photoconductivity resulting from G_{ac} and ϕ its phase shift referred to the excitation. All the quantities on the right hand side of Eq. (1) being known, Eqs. (1)–(2) would offer an easy DOS spectroscopy by varying T and ω, provided c_n and μ_n were known and assuming for N_c the same value as for crystalline silicon. Since this is not the case, we should look for other experiments to estimate these transport parameters.

Eqs. (1)–(2) are derived assuming that the carrier contribution to the alternating current is controlled by trapping/release of carriers from the states at E_ω. This regime is obtained with high frequency

* Corresponding author.
E-mail address: longeaud@lgep.supelec.fr (C. Longeaud).

0022-3093/$ – see front matter © 2011 Elsevier B.V. All rights reserved.
doi:10.1016/j.jnoncrysol.2011.11.018

of excitation, hence its name: the high frequency (HF) MPC. If the frequency is lowered the carrier contribution is controlled by recombination and one reaches the low frequency (LF) regime of the MPC technique. In this regime we have shown that a DOS spectroscopy is also possible according to the following equations [7]

$$N(E_{fn}) = \frac{2G_{dc}}{k_B T}\frac{\tan(\phi)}{\omega}, \quad (3)$$

with

$$E_c - E_{fn} = k_B T \ln\left[\frac{q\mu_n N_c}{\sigma_{dc}}\right], \quad (4)$$

E_{fn} being the position of the electron quasi Fermi level and σ_{dc} the steady-state photoconductivity.

The reader can note that if both techniques, HF- and LF-MPC, are applied to the same sample, by adjusting both the energy scales and the DOS it should be possible to estimate c_n and μ_n. However, experimentally we have found that there was often a temperature range in which $\tan(\phi)$ was negative and therefore the LF-MPC DOS spectroscopy was impossible.

The reason for this behavior was found after a study of the SSPC technique. This experiment is well known for the relation between σ_{dc} and G_{dc}: $\sigma_{dc} \propto G_{dc}^{\gamma}$. For some semiconductors one may observe $\gamma > 1$ in some temperature range, a situation detailed by Rose and called sensitization [8]. This phenomenon occurs when different types of states with different capture coefficients are present in the gap. A new analysis of the MPC experiment in the LF regime has shown that if the gap states are such that the sensitization phenomenon occurs then, in a given range of temperature close to that in which the sensitization appears, one may observe a negative phase shift instead of a positive one [9].

The SSPG technique was designed by Ritter *et al.*[2] to estimate the minority carrier diffusion length L_d. In this experiment the sample is illuminated by two laser beams, interfering if they are both vertically polarized or just superimposing if the polarizations are crossed. The grating spacing Λ is fixed by the angle between the beams and one records the variations of the ratio β of the current flowing in the sample with and without interferences as function of Λ to deduce the L_d value.

The SSPG configuration can be used to perform measurements adding a temporal variation to the excitation as in the moving grating technique (MGT) [3] or the modulated photocarrier grating (MPG) [4] techniques. Using the same set-up as for SSPG, placing an Electro-Optic Modulator (EOM) on the trajectory of one beam, the phase of the light can be modulated, the resulting intensity of the light impinging the surface of the film being

$$I(x,t) = I_1 + I_2 + 2\sqrt{I_1 I_2}\cos\left(\frac{2\pi x}{\Lambda} \pm \omega t\right), \quad (5)$$

where I_1 and I_2 are the respective intensities of each light beam, x the space coordinate, ω the angular frequency driving the EOM and the plus sign is for the first half of a period and the minus sign for the second half. According to Eq. (5) the grating is periodically moving with a constant velocity in one direction for half a period and in the other direction for the second half of the period. The current density δJ_{OPG} flowing in the film as a result of this oscillating photocarrier grating (OPG) can be measured with a lock-in amplifier synchronized at the frequency of the signal driving the EOM.

2.2. Experimental results

MPC and SSPC experiments were performed on a polymorphous a-Si:H film deposited onto a glass substrate and fitted with two parallel ohmic electrodes 1 mm apart. Details on the deposition conditions can be found in ref. [10] (sample #803242).

The LF-MPC was performed illuminating the sample with red light emitting diodes ($\lambda = 650$ nm) at a high G_{dc} of the order of 3×10^{19} $cm^{-3}\,s^{-1}$, in a frequency range 1–300 Hz, and varying the temperature in the 100–450 K range in 10 K steps. Two data treatment procedures were applied, a first one in which the DOS was deduced from the slope of $\tan(\phi)$ versus ω at low ω values, and a second treatment in which the DOS was deduced from the first *positive* slope of the variation of $\tan(\phi)$ versus ω. The HF-MPC was achieved with the same red light as for the LF-MPC, with G_{dc} of the order of 10^{17} $cm^{-3}\,s^{-1}$ and G_{ac} 3 times lower. The frequency of the modulation was varied in the range 12 Hz–40 kHz, and the temperature was varied from 450 K to 120 K in 30 K steps. For both experiments, each data point for a couple (ω, T) is the average of 10 successive measurements, one each second, and the error was estimated to be of the order of $\pm 8\%$ of the average value.

The SSPC measurements were performed with the same light source and the same generation rate as for LF-MPC to check for the occurrence of a sensitization.

In Fig. 1, we show the Nc/μ values (open diamonds) obtained for different couples (ω, T) in the HF-MPC experiment. We shall recall that the DOS shape is given by the upper envelope of all the spectra obtained at different T, one for each color. The departure of the spectra from the upper envelope originates from the influence of G_{dc} as shown elsewhere [6]. The DOS is made of a conduction band tail (CBT) visible at low energies, probed at low T, and deep states at higher energies, probed at high T. In the LF-MPC technique (circles in Fig. 1) we determine the N values (Eq. (3)) and at low T we may assume that LF-MPC and HF-MPC are probing only the CBT. We have then adjusted the $c_n N_c$ and $\mu_n N_c$ parameters, following Eqs. (1–4), so as to obtain the same Nc/μ in the CBT region for both experiments. The final values are displayed in Fig. 1 and the energy scales coming from Eqs. (2) and (4) were fixed according to this. It can be seen that the Nc/μ obtained at high T for both experiments do not match. This indicates that the deep states capture coefficient is clearly different from that of the CBT. To obtain a good match, at say 0.6 eV, between the Nc/μ determined from the HF-MPC and the Nc/μ calculated from the N values of the LF-MPC we should choose a c approximately ten times lower. In between the CBT and the deep states we obtained negative values of the phase shift in the LF-MPC experiment. This peculiar region is shown by open circles and N was calculated taking the first positive values of $\tan(\phi)$. This behavior indicates that the studied film presented a sensitization phenomenon in a given range of temperature, a result confirmed by the SSPC measurements giving γ values higher than one for temperatures in between say 200–260 K.

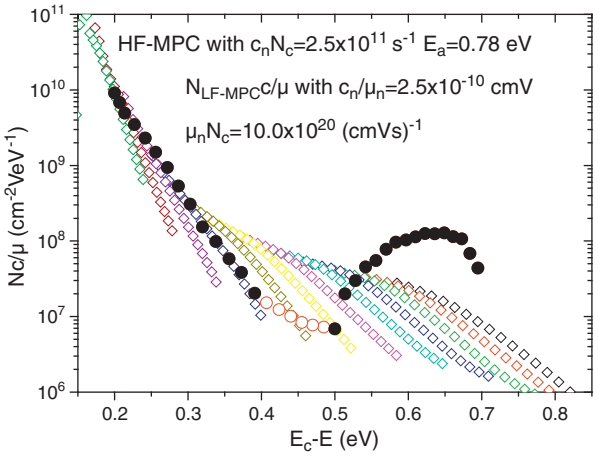

Fig. 1. Nc/μ determined from HF-MPC (open diamonds) and LF-MPC (circles) measurements. Error bars are within the size of a symbol.

It can be also seen that the energy at which all the Nc/μ curves drop is in agreement with the activation energy $E_a = 0.78$ eV measured from an Arrhenius plot of dark conductivity.

Concerning the OPG technique the experiments were performed at $T = 300$ K with a 1 μm thick undoped a-Si:H film deposited onto a glass substrate. Two parallel aluminium ohmic electrodes, 1 mm apart, were deposited on top of the film. Fig. 2 displays the variations of δJ_{opg} vs ω measured for two different external electric fields ξ_{ext} applied to the sample: $\xi_{ext} = 0$ and $\xi_{ext} = 40$ V/cm. The generation rate was equal to $G_{dc} = 4\times10^{20}$ cm^{-3} s^{-1} and the grating period equal to $\Lambda = 8.6$ μm. A clear maximum appears on the curve $\delta J_{OPG}(\omega)$ that we shall explain in the next section. Each data point is the average of 90 acquisitions, one each second, and the error was estimated to be ±5% of the mean value.

3. Discussion

The results of the MPC experiments can be summarized the following way. Matching the LF-MPC and HF-MPC in the CBT region leads to $c_n = 10^{-8}$ cm^{-3} s^{-1} and $\mu_n = 40$ cm^2 V^{-1} s^{-1} (assuming $N_c = 2.5\times10^{19}$ cm^3), two reasonable values expected for a-Si:H. Considering the LF-MPC and HF-MPC results for the deep states ($E_c - E > 0.5$ eV), from the comparison of the Nc/μ one can estimate the value of the capture coefficient ($c_{ndeep} \approx 1\times10^{-9}$ cm^{-3} s^{-1}) as well as the shape and magnitude ($N_{max} \approx 5\times10^{17}$ cm^{-3} eV^{-1}) of the $N(E_c - E)$ distribution of these states. Some other parameters can be experimentally deduced, as for instance the characteristic temperature T_c of the CBT ($T_c \approx 275$ K) or the dark Fermi level position ($E_c - E_{fn} \approx 0.78$ eV). The reader can note that according to the state distributions deduced from the LF-MPC a gap appears between the CBT and the deep states (0.35 eV$< E_c - E <0.5$ eV) that is not seen in the HF-MPC. This suggests that there exist in this energy range a distribution of states with low N values but high capture coefficient to give the proper Nc/μ values measured in HF-MPC.

To check these assumptions we have developed numerical calculations simulating the HF and LF-MPC experiments. The user can introduce DOS distributions and transport parameters (mobilities, band gap, …) and choose 'experimental' parameters as G_{dc} and the temperature range. The results of the calculation are treated as experimental results afterward. We present in Fig. 3 the distributions of states introduced in this numerical calculation along with the capture coefficients, some of them (in bold) coming directly from the experimental results.

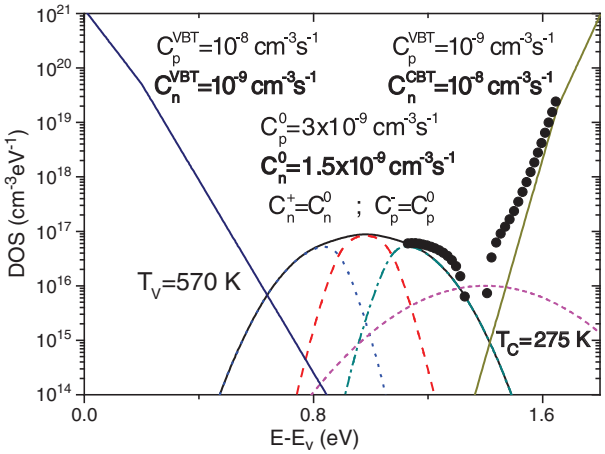

Fig. 3. DOS introduced in the numerical simulation to reproduce the experimental results (lines). As a matter of comparison the simulated results for the LF-MPC are shown (symbols).

We have introduced two band tails and deep states made of a defect pool [11] around the Fermi level and a low acceptor state centred at $E - E_v = 1.4$ eV with a high electron capture coefficient of the order of 10^{-7} cm^{3}eV^{-1} (for more details see [10]). Fig. 4 displays the results of the simulation of the HF-MPC and LF-MPC techniques. It is clear that the analogy with the experimental results is excellent. We are therefore quite confident on the potentialities of the techniques described above to provide a good insight of the a-Si:H properties and knowledge of its transport properties.

Concerning the OPG techniques we can explain the experimental results of Fig. 2 the following way. The light grating impinging the sample creates several arrays, in particular an array of free carriers $n(x)$ and an array of trapped carriers $N_{trap}(x)$. With a large Λ, $N_{trap}(x)$ does not vanish by diffusion and eventually creates a space charge array that results in an internal electric field array $\xi_{int}(x)$. With a static grating $n(x)$ and $\xi_{int}(x)$ are in quadrature, implying that the current is null if $\xi_{ext} = 0$ V/cm. When the light array is moving along the film surface, the free carriers grating follows it almost instantaneously, whereas the space charge array lies behind due to the necessary delay the trapped carriers need to reorganize. The $n(x)$ and $\xi_{int}(x)$ arrays are no longer in quadrature and a current may appear from the movement of free carriers in the internal field, that is even

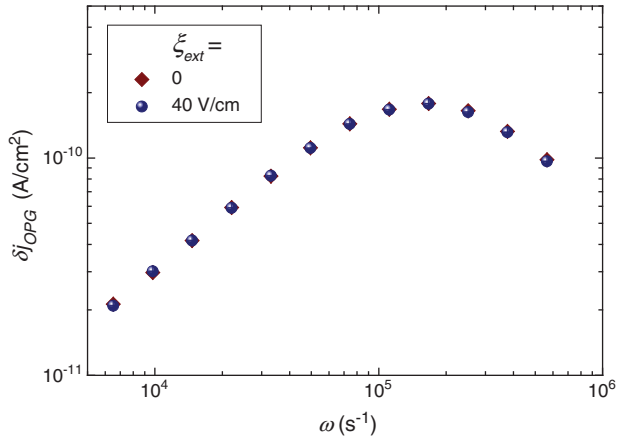

Fig. 2. δJ_{OPG} vs ω of the signal applied to the EOM, for an external electric field equal to zero (diamonds) and equal to 40 V/cm (circles). Error bars are within the size of a symbol.

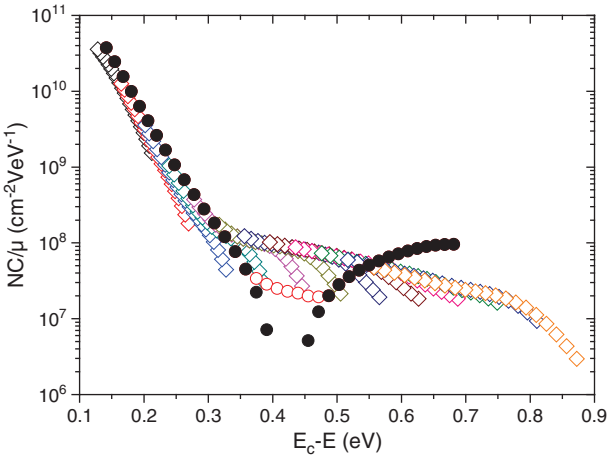

Fig. 4. Reproduction with a numerical calculation of the experimental results displayed in Fig. 1 (same symbols).

though $\xi_{ext} = 0$ V/cm. With a low external electric field applied, the alternating current is still mainly due to the internal field and one obtains the same variations of δJ_{OPG} vs. ω as with zero field applied (see Fig. 2).

As ω increases the velocity of the light grating increases too, and the phase lag between $n(x)$ and $\xi_{int}(x)$ tends to decrease, resulting in a steady increase of the OPG current. However, if the time needed for the light to cover Λ becomes too small, the trapped charges do not have time to reorganize and to follow the light array. The space charge array starts to blur, and the result is a decrease of the local internal field. The competition between the decrease of the phase shift between $n(x)$ and $\xi_{int}(x)$, and the blurring of the space charge, eventually ends with a decrease of the OPG current density with increasing ω. Therefore, the maximum of the $\delta J_{OPG}(\omega)$ curve, obtained for ω_{max}, must be linked to a characteristic time of the material.

Several characteristic times can be considered: the dielectric relaxation time τ_{diel}, the free electron lifetime τ_n and the small signal lifetime τ'_n, that is the lifetime of the excess free plus trapped electrons created by a small increase δG_{dc} of the generation rate. To find out to which time corresponds the maximum of the $\delta J_{OPG}(\omega)$ curve, we have developed numerical calculations simulating the OPG technique, calculations in which we have introduced the same distributions and parameters as those shown in Fig. 3.

We have reproduced all the experimental behaviors, as those displayed in Fig. 2, calculated all the characteristic times and compared them to $1/\omega_{max}$. We present in Fig. 5 the variations of these times with the generation rate G_{dc}. At low generation rates we observe that $1/\omega_{max}$ is close to τ_{diel} whereas at high generation rates $1/\omega_{max}$ is close to τ'_n. These two cases correspond to the well-known dielectric and lifetime regimes, the transition between them being indicated by a vertical dashed line in Fig. 5.

The knowledge of τ'_n is very interesting because, being this time linked to the trapped carriers, we expect to extract information on the DOS from it. To illustrate this point we can perform a simple calculation considering that the DOS distribution is made of monovalent states. An expression of τ'_n is

$$\tau_n' = \frac{\partial n^{tot}}{\partial G_{dc}} = \frac{\partial \left[n_0 + \int f_0 \; N^{ACC} \; dE \right]}{\partial G_{dc}}, \tag{6}$$

in which n^{tot} is the total concentration of electrons, i.e. the free (n_0) plus trapped concentrations, f_0 the occupation function and N^{ACC} the density of acceptor states. For a given G_{dc} one can calculate the position of the electron quasi Fermi level E_{fn} from Eq. (4). Taking account of the power–law relationship between photoconductivity and G_{dc}, $\sigma_{dc} \propto G_{dc}^{\gamma}$, a straightforward calculation, based on the derivative of Eq. (4), leads to

$$\partial G_{dc} = \frac{G_{dc}}{k_B T \; \gamma} \partial E_{Fn}. \tag{7}$$

Usually, in disordered semiconductors, the density of trapped carriers is much larger than the density of free carriers, and we can neglect n_0 in Eq. (6). Another straightforward calculation leads to

$$\left. \frac{\partial n^{tot}}{\partial E} \right|_{E=E_{Fn}} = \frac{G_{dc0} \; \tau_n'}{k_B T \; \gamma} = f_0(E_{Fn}) \; N_{trap}(E_{Fn}). \tag{8}$$

Eq. (8) coupled with Eq. (4) allows a DOS spectroscopy if the experiment is performed at different temperatures, provided $f_0(E_{fn})$ is known. Electrons being the majority carriers in a-Si:H, an abrupt simplification is: $f_0(E_{fn}) = 1$.

Calculations of τ'_n and γ were achieved with our simulations for temperatures ranging from 100 to 460 K with a generation rate of $G_{dc} = 10^{21}$ cm^{-3} s^{-1}. The OPG-DOS spectroscopy based on the oversimplified Eq. (8) is displayed in Fig. 6 (circles), where the general trends of the original DOS (full lines) are well reproduced but the precision is rather poor.

The OPG-DOS spectroscopy can be refined if one calculates a proper value for the coefficient $f_0(E_{fn})$. Let us consider the CBT probed at low temperatures. Starting from the expression of the occupation function under illumination given in ref. [12], after some simplifications one ends with

$$f_0(E) = \frac{1}{1 + \exp\left({}^{(E-E_{fn})}/_{k_B T} \right)}. \tag{9}$$

Assuming that the CBT is exponentially decreasing from the band edge with a characteristic temperature T_c, the derivation of concentration of trapped electrons in the CBT with respect to E_{fn} gives, after simple calculations,

$$\frac{\partial N_{trap}}{\partial E_{fn}} = N_{trap}(E_{fn}) \int \frac{\exp(x\alpha)}{[1 + \exp(x)]^2} dx, \tag{10}$$

writing $x = {}^{E-E_{fn}}/_{k_B T}$, and $\alpha = 1 + {}^{T}/_{T_c}$. If α is lower than 2 (for temperatures lower than T_c) the integral is equal to $\frac{(1-\alpha)\pi}{\sin(\alpha\pi)}$, giving the exact value of $f_0(E_{fn})$. Consequently, for measurement temperatures below say 200 K, we can imagine a recurrent procedure to determine

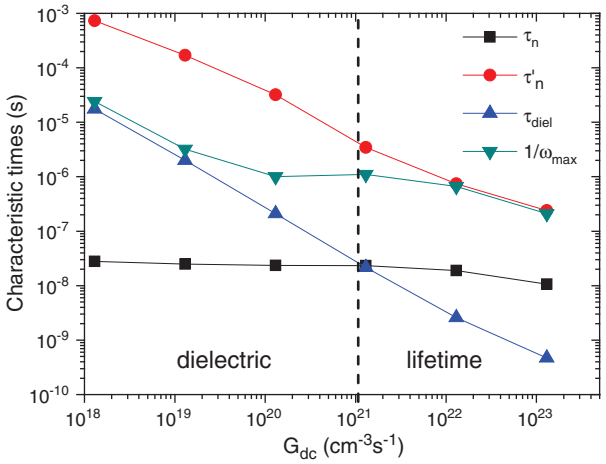

Fig. 5. Calculated results showing the evolution of different characteristic times with the generation rate G_{dc} at $T = 300$ K (lines are guide to the eye).

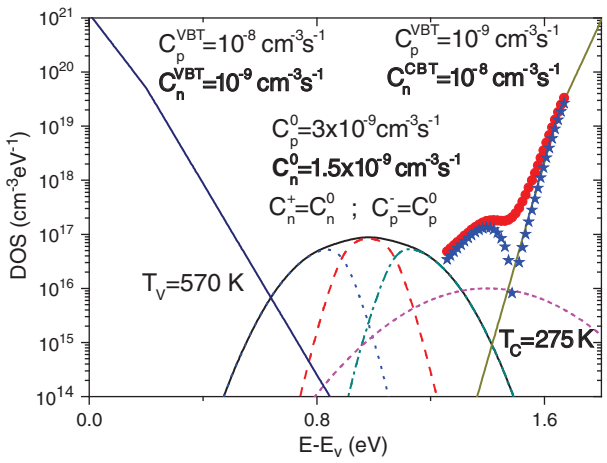

Fig. 6. DOS spectroscopy from the OPG technique with a simple procedure (circles) or after correction (stars). Full lines display the original DOS.

the shape of the band tail: assuming a T_c, correcting the simplified OPG-DOS values with the above expression, checking if the final T_c determined from the corrected values of the OPG-DOS is the same as the introduced one and repeating this procedure until there is a convergence. For higher measurement temperatures we can subtract this contribution to the total contribution of the estimated DOS. Following this procedure we find the OPG-DOS displayed by stars in Fig. 6. The agreement with the introduced CBT is excellent but not really satisfying concerning the deep states for which we obtain the proper magnitude but not the proper distribution. This behavior is due to the fact that we are dealing with amphoteric states. In this case we probe the D^0/D^- contribution and more work is needed to check if a proper spectroscopy of the deep states is possible.

However, transport parameters can be extracted by comparing the results obtained from the OPG and HF-MPC techniques when probing the CBT states, exactly as we did with the HF-MPC and LF-MPC. The OPG technique is an alternative to the LF-MPC technique in this respect. As far as the deep states are concerned, though we still have to investigate on the possibility to achieve a DOS spectroscopy of the deep states if they are amphoteric, the OPG technique allows the determination of an order of magnitude of the D^- concentration, a piece of information that was not available up to now.

4. Conclusion

We have reviewed some of the existing techniques based on the photoconductivity properties of a-SiH. In addition to the achievement of DOS spectroscopies for some of them, we have shown that many parameters can be deduced by cross checking their respective results. We have also described a new technique based on the same set-up as the SSPG that, combined with measurements of γ, provides an easy means to perform a DOS spectroscopy of the CBT. We have shown theoretically that the determination of the CBT DOS is really accurate and that we may estimate the D^- concentration. Besides, combined with other experiments as MPC, it should lead to the determination of important a-Si:H transport parameters such as the extended states mobility and CBT capture coefficient. Experiments are under way to check all the potentialities of this technique.

Acknowledgements

This work was partly supported by ECOS-Sud under project A08E01.

References

[1] H. Oheda, J. Appl. Phys. 52 (1981) 6693–6700.
[2] D. Ritter, E. Zeldov, K. Weiser, Appl. Phys. Lett. 49 (1986) 791–793.
[3] U. Haken, M. Hundhausen, L. Ley, Appl. Phys. Lett. 63 (1993) 3066–3068.
[4] K. Hattori, Y. Koji, S. Fukuda, W. Ma, H. Okamoto, Y. Hamakawa, J. Appl. Phys. 73 (1993) 3846–3851.
[5] R. Brüggemann, C. Main, C. Berkin, J. Reynolds, Philos. Mag. B 62 (1990) 29–45.
[6] C. Longeaud, J.P. Kleider, Phys. Rev. B 45 (1992) 11672–11684.
[7] M.E. Gueunier, C. Longeaud, J.P. Kleider, Eur. Phys. J. Appl. Phys. 26 (2004) 75–85.
[8] A. Rose, Concepts in photoconductivity and allied problems, Wiley & sons, New York, 1966.
[9] J.A. Schmidt, C. Longeaud, R.R. Koropecki, R. Arce, J. Appl. Phys. 101 (2007) 1037051–10370510.
[10] C. Longeaud, J.A. Schmidt, R.R. Koropecki, Phys. Rev. B 73 (2006) 2353171–23531710.
[11] M.J. Powell, S.C. Deane, Phys. Rev. B 48 (1993) 10815–10827.
[12] G.W. Taylor, J.G. Simmons, J. Non-Cryst. Solids 8–10 (1972) 940–946.